Dioxirane. Its synthesis, microwave spectrum, structure, and dipole moment

ARTICLE *in* JOURNAL OF THE AMERICAN CHEMICAL SOCIETY · APRIL 1978

Impact Factor: 12.11 · DOI: 10.1021/ja00484a034

2 AUTHORS:

R.D. Suenram
University of Virginia
247 PUBLICATIONS **6,838** CITATIONS
SEE PROFILE

Francis J. Lovas
National Institute of Standards and Technology
287 PUBLICATIONS **9,234** CITATIONS
SEE PROFILE

Dioxirane. Its Synthesis, Microwave Spectrum, Structure, and Dipole Moment

R. D. Suenram* and F. J. Lovas

Contribution from the National Bureau of Standards, Washington, D.C. 20234. *Received January 4, 1978*

Abstract: Dioxirane, $H_2\overline{COO}$, has been identified in the reaction of ozone with ethylene at low temperature. The methods employed in synthesizing several isotopic forms of dioxirane and measurement of their rotational spectra are described. The moments of inertia obtained for $H_2{}^{12}\overline{C^{16}O^{16}O}$, $HD{}^{12}\overline{C^{16}O^{16}O}$, $H_2{}^{13}\overline{C^{16}O^{16}O}$, and $H_2{}^{12}\overline{C^{18}O^{18}O}$ were employed in obtaining the following r_s structure: r_{HC} = 1.0903 (18), r_{CO} = 1.3878 (38), r_{OO} = 1.5155 (28) Å; $\angle_{HCH}$ = 117.32 (20), $\angle_{OCO}$ = 66.19 (18)°. The electric dipole moment, μ_b = 2.479 (70) D, was determined from Stark effect measurement on the $H_2{}^{12}\overline{C^{16}O^{16}O}$ species.

Introduction

The ability of ozone to attack olefinic double bonds in hydrocarbon compounds has been known for some time. Studies of this reaction sequence can be traced back to the early part of this century.[1,2] In the early 1950s Criegee studied the reaction sequence in detail and in 1957 he published his now classic paper on the mechanism of ozonolysis of olefins.[3] In this paper he postulated the mechanism (1). In this mechanism,

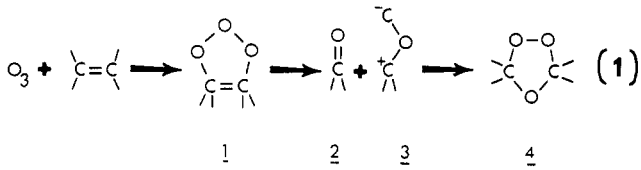

(1)

1 2 3 4

the first step involves the simple addition of ozone across the double bond to form a primary ozonide or "molozonide" (**1**). This adduct is generally quite unstable and decomposes readily into an aldehyde and a "zwitterionic" intermediate generally known as the Criegee intermediate (**3**). In solution these two fragments readily recombine to form a secondary ozonide (**4**). Subsequent to these fundamental studies, variations in the mechanistic routes have been proposed to explain the reaction which are only slight modifications of the mechanism proposed by Criegee.[4-6] In the early 1960s the gas phase ozone-olefin reaction was recognized as one of the prime reaction sequences participating in photochemical smog formation over urban areas.[7] At this point many new investigations of this reaction sequence were initiated to gain a fuller understanding of the reaction mechanism.

The majority of the studies that have been carried out can be broken down into three broad areas of interest. The early work, for the most part, focused on reactions in solution and the goal of these investigations was elucidation of the reaction mechanism and development of new synthetic routes. Later work, carried out primarily by Kuczkowski, Gillies and coworkers, was aimed at the structural determination of some of the smaller ozonides.[6,8] In addition to the structural information which these workers obtained, their isotopic substitution studies provided some excellent insights into the mechanism of the solution reaction. Some of the more recent work, where air pollution was the major concern, dealt with reaction rates of the various steps of the reaction sequence. These investigations were carried out using reactants in the gas phase.

In spite of all the previous investigations, there is still much about the reaction sequence that is not well quantified. This is especially true of the early stages of the reaction where the highly unstable primary ozonide and the Criegee intermediate are thought to be present but not directly observed. The goal of this investigation was to devise a means whereby the early stages of the reaction could be slowed down and controlled to the point where some of the reaction products that were present in the early stages could be observed directly. The results of this attempt are presented in the following sections.

Although a variety of experimental techniques have been employed in the investigation of ozone-olefin systems, most procedures either involve a low temperature ozonolysis in solution followed by warming the resultant mixture and separation and identification of the end products, or room temperature studies of the gas phase reaction. NMR and IR studies of the reaction at low temperatures indicate that in the range of −130 to −80 °C changes generally occur that are attributed to the decomposition of the primary ozonide.[9,10]

Our approach was to design a microwave absorption cell which could be used as a low temperature reactor in order to study the reaction as a function of temperature by observing the microwave spectra of the various products present in the gas phase at different temperatures.

Experimental Section

A. Stark Cell and Vacuum Systems. Mixtures of ozone and olefins tend to be explosive and ozone and ozonides in general are quite reactive especially toward organic compounds. In the design of the absorption cell and sample handling system, these characteristics were allowed for by constructing the entire system of stainless steel, Pyrex and Teflon. A 1-m Stark cell of conventional design was built from thin wall stainless steel waveguide (WR62, 12.4-18.5 GHz), Figure 1. In forming the vacuum seals, Teflon O-rings and windows were used throughout. This type of seal alleviates the need for any grease or rubber materials to be used in forming the vacuum seals. Two ground-glass joints in the inlet system were lubricated with Kel-F grease. Instead of using the normal liquid nitrogen cooled trap in front of the vacuum pump, the trap was filled with copper turnings and heated to ~100 °C. The copper turnings are excellent for destroying ozone and other reactive compounds that are formed in the reaction. This method of product removal lessens the possibility of explosions occurring that could result from an accumulation of materials in a liquid nitrogen cooled trap.

B. Cooling Cylinder. In order to cool the cell to liquid nitrogen temperatures, a cooling cylinder was constructed from stainless steel pipe with an inner diameter just large enough to slip over the end blocks of the cell; see Figure 1. Three flow ports of 0.5-in. diameter were welded to the side of the pipe, one near each end and one in the center. Teflon end plugs were machined to make a snug fit with the waveguide and O-ring seals provided a tight fit between the Teflon plugs and the pipe. To moderate the rate of warming, once liquid nitrogen cooling was discontinued, rubber steam pipe insulation was taped over the outside of the steel cylinder. To cool the cell, liquid nitrogen was usually added at the center flow port and allowed to boil off through the end flow ports. With cooling apparatus in place, the cell could be cooled to −196 °C with ease. Self-warming to room temperature required ~1.5 h. The temperature of the cell was moni-

Table I. Observed Transition Frequencies for Dioxirane[a]

Transition $J'_{K'_{-1}K'_{+1}} - J''_{K''_{-1}K''_{+1}}$	$H_2C^{16}O^{16}O$ Obs ν	σ[c]	Δν[d]	$H_2{}^{13}C^{16}O^{16}O$ Obs ν	σ	Δν	$HDC^{16}O^{16}O$ Obs ν	σ	Δν	$H_2C^{18}O^{18}O$[b] Obs ν	σ	Δν
$3_{30} - 3_{21}$	27660.90(20)[e]	0.139	-0.120							35623.30(30)[e]	0.614	1.483
$3_{21} - 3_{12}$	29938.05(05)	0.109	0.246	30123.85(05)[e]	0.066	0.003	29344.24(30)[e]	0.137	-0.070	28216.16(40)	0.373	0.241
$7_{70} - 7_{61}$							30073.97(06)	0.259	-0.057			
$9_{81} - 9_{72}$							30223.59(06)	0.219	-0.092			
$4_{31} - 4_{22}$	30872.02(20)	0.081	0.230	29640.53(10)	0.051	0.088	28119.28(30)	0.149	0.141	33418.42(50)	0.430	0.468
$4_{22} - 4_{13}$										45551.84(36)	0.856	0.766
$2_{11} - 2_{02}$	31753.01(05)	0.128	0.045	32136.43(08)	0.085	0.038	30523.84(50)	0.149	-0.145	28487.40(08)	0.460	-1.149
$5_{41} - 5_{32}$	35866.17(50)	0.117	0.187	31735.05(08)	0.070	0.272	27114.29(30)	0.176	-0.118	45543.44(36)	0.848	-1.148
$4_{40} - 4_{31}$				32294.62(10)	0.105	-0.081						
$2_{21} - 2_{12}$	42589.61(26)	0.113	0.046				33461.21(18)	0.167	0.001			
$7_{52} - 7_{43}$				44962.26(16)	0.094	0.091						
$3_{31} - 3_{22}$				45207.53(08)	0.087	-0.110	35006.60(18)	0.144	0.054			
$6_{42} - 6_{33}$	45541.15(20)	0.130	-0.070	47184.67(06)	0.093	0.098						
$8_{62} - 8_{53}$				45682.51(08)	0.100	-0.148						
$7_{61} - 7_{52}$				46182.40(04)	0.120	0.081						
$6_{51} - 6_{42}$	45663.92(12)	0.175	-0.301									
$10_{91} - 10_{82}$							33666.74(18)	0.252	0.068			
$9_{63} - 9_{54}$	59995.68(30)	0.267	-0.027									
$9_{72} - 9_{63}$	63095.60(24)	0.275	0.042	50217.48(04)	0.128	-0.031						
$5_{32} - 5_{23}$				51027.12(08)	0.103	-0.148						
$4_{41} - 4_{32}$				51610.23(08)	0.090	0.000	37088.35(15)	0.133	0.263			
$4_{32} - 4_{23}$	63931.40(50)	0.211	0.167									
$1_{11} - 0_{00}$							39160.36(10)	0.131	-0.262			
$5_{51} - 5_{42}$	68231.55(50)	0.149	0.092				39715.40(50)	0.172	-0.038			
$2_{02} - 1_{11}$	68470.19(50)	0.158	-0.038				66093.90(40)	0.178	0.567			
$6_{60} - 6_{51}$	73277.80(50)	0.251	-0.007									
$2_{12} - 1_{01}$	73316.02(50)	0.166	0.577				67166.30(100)	0.176	-0.376	69066.10(10)	0.856	-0.585
$3_{12} - 2_{21}$	115175.10(30)	0.229	-0.095	116147.71(10)	0.142	0.058	111418.10(17)	0.211	-0.081			
$3_{22} - 2_{11}$							117478.10(42)	0.211	0.050			
$2_{20} - 1_{11}$	119264.15(21)	0.193	-0.457	117208.10(10)	0.144	-0.051				112025.90(90)	0.856	0.586
$4_{04} - 3_{13}$	130247.09(69)	0.196	-0.026									
$4_{14} - 3_{03}$	130406.02(46)	0.196	0.055	128148.62(21)	0.148	-0.018	122665.65(50)	0.277	-0.007			

[a] All values are given in MHz. [b] Results of a rigid rotor fit. [c] Standard deviation. [d] Observed minus calculated. [e] The numbers in parentheses are the measured uncertainties in transition frequency and refer to the last two digits given.

tored by three thermocouples taped to the outside wall of the waveguide.

C. Instrumental. The spectrometer used was of conventional design employing 80-kHz Stark modulation.[11] For the initial experiments a backward wave oscillator was used to rapidly scan a portion of the spectral range of interest. Once the overall characteristics of the spectrum had been mapped out, free running reflex klystrons were used to obtain precise frequency measurements of the molecular absorption lines.

D. Ozone Storage and Handling. Ozone is an explosive substance and its storage and handling requires a certain amount of care. A convenient method for storing ozone is to trap it on silica gel.[12] A silica gel trap provides a readily available, convenient source of fairly pure ozone and it eliminates the necessity of preparing it fresh every time an experiment is run.

Spectral Observations

A. Method of Observation. A number of variations on the procedure for introducing ethylene and ozone into the waveguide was attempted. As it turned out it was quite difficult to get both reactants into the cell at liquid nitrogen temperature without an explosion occurring. Eventually the best procedure that was found was to pressurize the cell with ~1 Torr of ozone, cool the cell to −196 °C with liquid nitrogen, and pump off any residual oxygen that did not freeze out and then allow ethylene to bleed into the cell through a needle valve for ~15 s, keeping the pressure between 50 to 100 mTorr in the inlet lines. This allowed the ozone to form a thin layer over a large area of the inside of the cell and thus prevented any localized buildup of ozone and ethylene. It should be emphasized at this point that during the course of this work many variations on this procedure were used and the general observation was that the ratio of reactants was not critical with respect to dioxirane formation as long as some of each were introduced into the cell and no explosion occurred. Once the reactants were in the cell, cooling was discontinued and the warming process allowed to begin. Spectral scans were initiated immediately and repeated every few minutes as the cell warmed; see Figure 2. This procedure was repeated several times for each frequency region in order

Table II. Rotational Constants and Centrifugal Distortion Parameters for Dioxirane

	$H_2\overline{COO}$[a]	$H_2{}^{13}\overline{COO}$	$HD\overline{COO}$	$H_2\overline{C^{18}C^{18}O}$[b]
A'', MHz	28976.762 (78)[c]	28012.641 (68)	25157.48 (11)	28120.96 (21)
B'', MHz	25056.382 (86)	25056.772 (86)	24154.97 (10)	22491.83 (22)
C'', MHz	14779.889 (65)	14524.118 (75)	14003.461 (72)	13648.58 (23)
τ_1, MHz	−0.371 (60)	−0.422 (64)	−0.482 (65)	
τ_2, MHz	−0.106 (20)	−0.123 (22)	−0.147 (22)	
τ_3, MHz[d]	6.95 (16)	8.41 (26)	17.1 (13)	
τ_{aaaa}, MHz	−0.325 (18)	−0.323 (16)	−0.267 (23)	
τ_{bbbb}, MHz	−0.398 (19)	−0.418 (19)	−0.398 (23)	
τ_{cccc}, MHz	−0.043 (11)	−0.0582 (80)	−0.041 (10)	

[a] The parameters reported here are only slight refinements of those reported in ref 13 but are given here for completeness. [b] For the disubstituted ^{18}O species only the rigid rotor rotational constants are reported owing to the limited number of transition frequencies that were measured. [c] The numbers in parentheses represent one standard deviation of the corresponding parameters. [d] The value of τ_3 is fixed by setting R_6 = 0 (see ref 15).

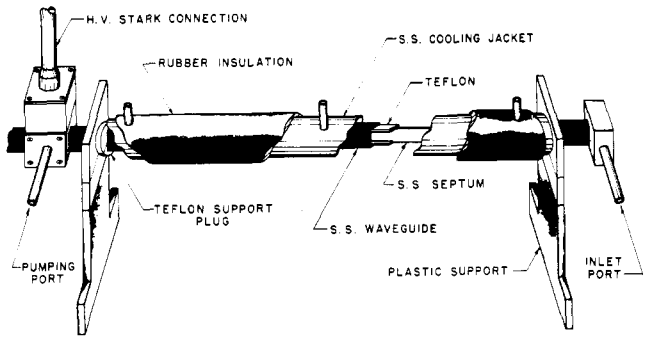

Figure 1. Schematic drawing of stainless steel septum absorption cell for low temperature microwave studies. See text for discussion of materials and construction.

to assure that the results were reproducible. Once a particular frequency region had been thoroughly mapped out, a new region was scanned.

Figure 2 shows the results of repetitive scans through the 29–31-GHz region. These survey scans were made using the phase locked backward wave oscillator with a scan rate of 6 MHz/s. The temperature at the beginning and end of each scan was recorded. In trace a (−158 to −133 °C) only ozone is observable in the gas phase in the cell. In trace b (−125 to −107 °C) ozone is still present and two transitions of formaldehyde (H_2CO) appear. In trace c (−100 to −84 °C) ozone and formaldehyde are still present but now two new transitions assigned to dioxirane[13] have grown in. In trace d (−81 to −69 °C) ozone, formaldehyde, and dioxirane are still present with the dioxirane lines now near maximum intensity. In addition a transition of ethylene oxide was identified as well as some smaller lines which belong to the secondary ozonide. In trace e (−63 to −57 °C) the spectrum of the secondary ozonide (SOZ) dominates, although transitions of all the other species can still be found. In trace f (−37 to −32 °C) the pressure has been reduced by pumping out the cell and only transitions from the secondary ozonide and formaldehyde are evident. The amplifier gain was also reduced by a factor of 2.5 for this trace. Scans throughout the remainder of R band (26.5–40 GHz) were made in a similar fashion. The details of the spectral assignment and molecular identification of dioxirane, $H_2\overline{COO}$, were reported previously[13] and will not be repeated here.

B. Synthesis and Spectra of Isotopic Species of Dioxirane. In order to determine the molecular structure and confirm the identification of dioxirane several isotopic forms of the compound were synthesized. The monodeuterated species was synthesized by using 99% enriched 1,2-dideuterioethylene as a reactant. The $H_2{}^{13}\overline{COO}$ species was prepared by using 90% enriched [1,2-^{13}C]ethylene. A sample of disubstituted ^{18}O dioxirane was made from $^{18}O_3$ which was generated from a small amount of 99% enriched $^{18}O_2$. The isotopically enriched ozone ($^{18}O_3$) was prepared in a static reactor using a tesla coil on the outside of the reaction vessel. Several grams of silica gel were placed in a trap and degassed in the usual fashion prior to admitting the enriched oxygen. In a typical preparation 10 Torr of $^{18}O_2$ was admitted to the 100-cm^3 trap which was cooled using a trichloroethylene–dry ice bath. Approximately 30 min of operation of the tesla coil was sufficient to transform the oxygen to ozone. The sample prepared in this manner was sufficient for several microwave experiments.

C. Measured Rotational Transitions. The measured transition frequencies of all the isotopic species studied are given in Table I. For all of the species studied, except the disubstituted ^{18}O species, a sufficient number of transitions have been measured to allow a centrifugal distortion analysis to be performed. For the ^{18}O species only a rigid rotor analysis could be carried out. The distortion analyses were carried out using the quartic distortion model of Watson[14] and computer program developed by Kirchhoff.[15] The rotational constants and distortion parameters are given in Table II.

Molecular Structure and Dipole Moment

A. Structure. Since all the atoms in the molecule have been isotopically substituted, a complete substitution (r_s) structure can be obtained using the method of Costain.[16] Kraitchman's equations[17] were employed in calculating the atomic coordinates for the carbon and hydrogen atoms, and a similar set of equations, which were derived specifically to accommodate double substitution in a molecule,[18,19] were employed in determining the oxygen coordinates. The substitution method has the virtue that some of the vibration-rotation effects are cancelled out since only differences in the moments of inertia are involved. The atomic coordinates and molecular parameters obtained are given in Table III. In the case of dioxirane there are no extremely small coordinates so the sign choice is unambiguous. The fact that there are no small coordinates also allows an accurate structure to be determined since the r_s method works best when all coordinates are >0.15 Å. The uncertainties associated with the atomic coordinates in Table III are those which arise solely from the uncertainties in the rotational constants in Table II. These uncertainties, while much smaller than the uncertainties associated with the vibration-rotation approximation, offer some estimate of the experimental precision of the data. More reasonable estimates of the true uncertainties in the molecular parameters are given by the Costain uncertainties which can be propagated from the atomic coordinates. For any given atomic coordinate (q_i) the Costain uncertainty is given by $\Delta q_i = 0.0015/q_i$. The final structural parameters and their associated uncertainties are shown in Figure 3.

B. Dipole Moment. The molecular dipole moment was derived from measurements of the frequency shift versus applied

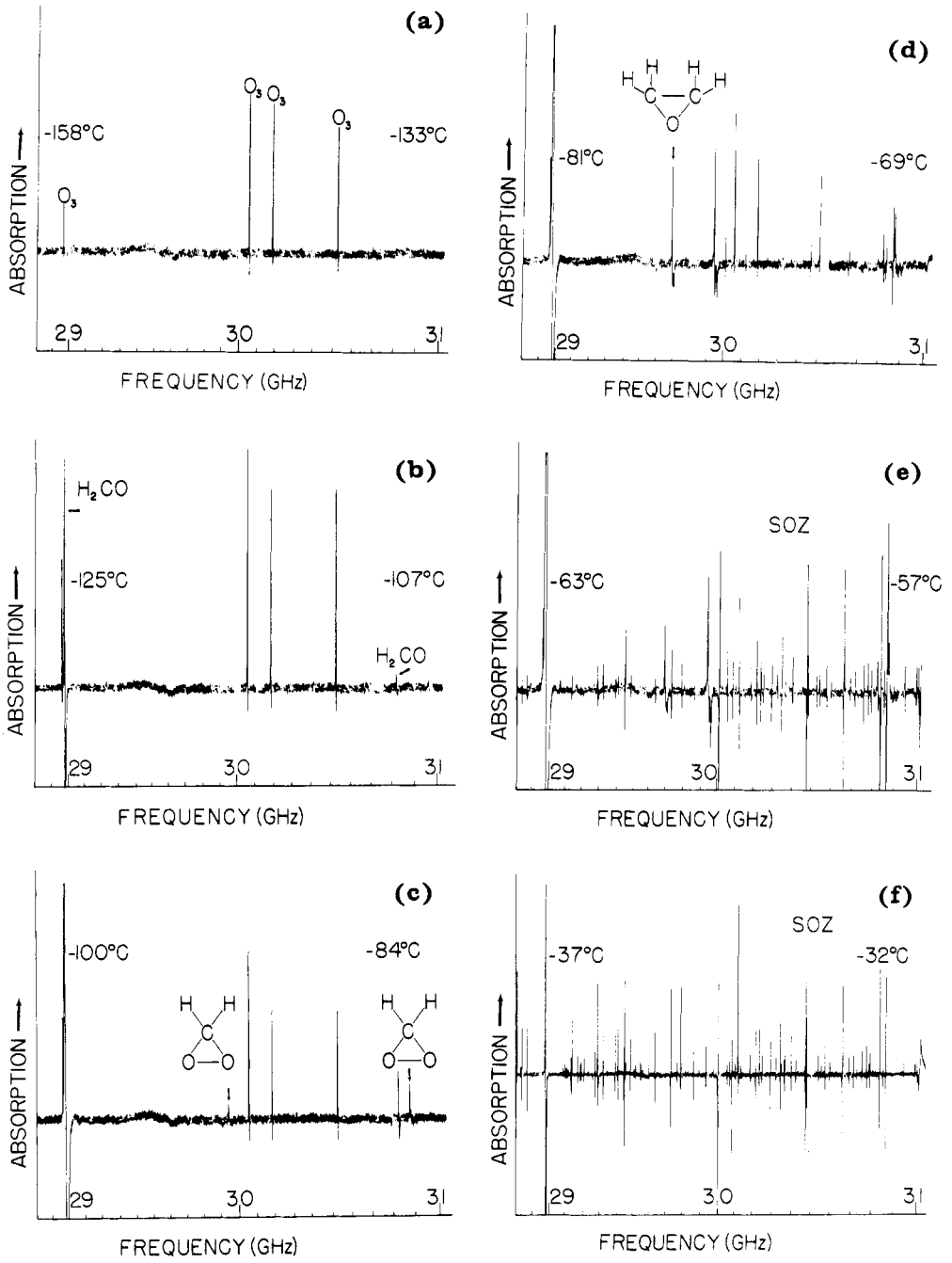

Figure 2. Microwave absorption spectra of the products of the low temperature reaction of ethylene with ozone. A series of spectra are shown in the range of 29 GHz with increasing absorption cell temperature which was measured at the beginning and end of each spectral scan. At the lowest temperature (a) only ozone rotational transitions are observed. In b both ozone and formaldehyde can be seen. In c two transitions of dioxirane are indicated and O_3 and H_2CO remain. In the next scan (d) the dioxirane lines are near maximum intensity and a transition of ethylene oxide is now evident. In the final two scans shown (e and f) the secondary ozonide (SOZ) begins to dominate, although in e the other products identified can still be observed. Between scans e and f the cell pressure was reduced by ~75% by pumping and the gain was reduced by 2.5 for scan f.

electric field for the $M = 2$ Stark component of the 2_{11}-2_{02} transition and the $M = 2$ and $M = 3$ Stark components of the 3_{21}-3_{12} transition. Four frequency and field measurements were made for each Stark component, thus providing 12 measurements of the unknown, μ_b. The data were least squares fit to

$$\Delta\nu = (a + bM^2)E^2\mu_b^2 \qquad (2)$$

where $\Delta\nu$ is the observed frequency shift at the applied electric field $E(E = V/d)$ where d is the distance from the cell septum to the cell wall determined by calibration with OCS (μ[OCS] = 0.71519 (3)).[20] The constants a and b are the usual second-order coefficients for the transition in question.[21] For the 2_{11}-2_{02} transition $a = -3.6837 \times 10^{-7}$ and $b = -1.3283 \times 10^{-7}$ were employed, and $a = -6.4115 \times 10^{-8}$ and $b = 2.2274 \times 10^{-7}$ were employed in eq 2 for the 3_{12}-3_{21} transition with units of MHz·cm^2·V^{-2}·D^{-2}. This analysis provides $\mu_b = 2.479$ (70) D.

Discussion

A. Structure. Since dioxirane is the first member of this new class of compounds, no comparison with other members of the class can be made at this time. However, one can compare the bond lengths with those of other compounds which contain typical C–O and O–O bonds. This is done in Table IV. The C–O bonds that were chosen for comparison were aliphatic bonds found in alcohols, ethers, and esters. In these compounds, the C–O bonds tend to be longer than that found in dioxirane.

Table III. Substitution Atomic Coordinates and Molecular Parameters for Dioxirane[a]

	a coordinate	*b* coordinate	*c* coordinate
H	0[b]	1.349670 (78)[c]	0.931240 (81)
C	0[b]	0.78258 (10)	0[b]
O	0.75777 (78)	−0.3801 (16)	0[b]

	bond lengths and angles	Costain uncert[d]
r_{CH}	1.09032 (12)	±0.0018
r_{CO}	1.3878 (15)	±0.0038
r_{OO}	1.5155 (16)	± 0.0028
∠HCH	117.320 (12)	±0.20
∠OCO	66.189 (67)	±0.18

[a] All distances are in ångstroms and angles are in degrees. [b] These coordinates have been set equal to zero as required by symmetry considerations. [c] The numbers in parentheses represent one standard deviation of the corresponding parameters which have been propagated from the rotational constants. [d] The Costain uncertainties are defined by $\Delta q_i = 0.0015/q_i$ where q_i is an atomic coordinate.

There are few peroxy bonds available for comparison, and the two shown in Table IV are shorter than the O-O bond in dioxirane. The abnormal lengths of the C-O and O-O bonds in dioxirane are undoubtedly a result of the strain that must be present in the ring.

B. Mechanism. That dioxirane might exist as an intermediate in the complex gas phase reaction between ozone and olefins was suggested by Ha et al.[23] and Wadt and Goddard.[24] Its discovery and importance in the reaction sequence have now been elucidated.[13,25] In a more recent publication Harding and Goddard[26] have expanded their theoretical calculations on the ozone-olefin system and suggested four possible reaction routes for the decomposition of the primary ozonide (A-D). Since

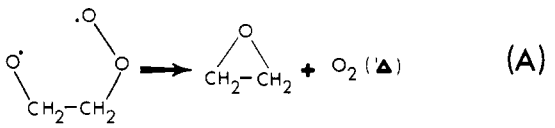

(A)

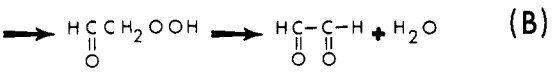

(B)

ethylene oxide has been observed in our low-temperature study (Figure 2) and by Kühne et al.[27] in reactions at room temperature, path A is viable. There is no evidence for the presence of any of the compounds in path B, although it is an intriguing possibility since it is energetically the most favorable by far ($\Delta H = -79$ kcal/mol).[26] The end product, glyoxal, is not easily observed via microwave techniques since it exists primarily in the nonpolar trans configuration. The α-peroxyacetaldehyde intermediate is an interesting molecular species whose spectrum is unknown. No evidence for any transitions of this compound was obtained in our experiments. Path C

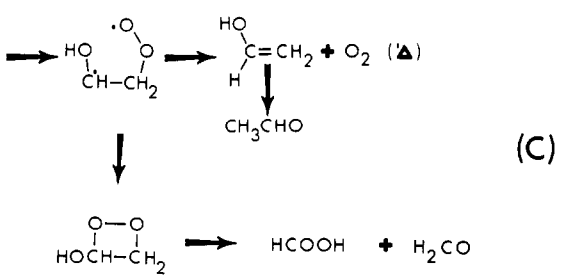

(C)

branches into two parts. The part leading to vinyl alcohol and acetaldehyde could be examined in our experiment because

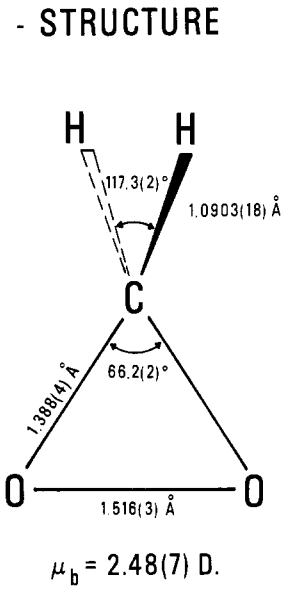

Figure 3. The molecular structure and dipole moment of dioxirane.

Table IV. Comparison of Bond Lengths Determined for Dioxirane with Those of Other Compounds

compd	r_{CO}, Å	r_{OO}, Å	type of expt[a]	ref
dioxirane	1.3878 (38)	1.5155 (28)	MW	This work
methanol	1.4246 (24)		MW	22, p 148
ethanol	1.4310 (50)		MW	22, p 203
dimethyl ether	1.410 (3)		MW	22, p 204
ethylene epoxide	1.431 (2)		MW	22, p 185
tetrahydrofuran	1.4280 (15)		ED	22, p 287
methyl formate	1.437 (10)		MW	22, p 185
hydrogen peroxide		1.467 (5)	IR	*b*
ethylene ozonide	1.416_e (2)	1.461 (2)	MW	*c*
	1.412_p (2)			

[a] MW = microwave, ED = electron diffraction, and IR = infrared. [b] P. A. Giguère and T. K. K. Srinivasan, *J. Mol. Spectrosc.*, **66,** 168 (1977). [c] R. L. Kuczkowski, C. W. Gillies, and K. L. Gallaher, *ibid.*, **60,** 361 (1976).

the microwave spectra of these molecular species are strong and well known. No transitions from either species could be observed. The second branch which passes through a dioxetane intermediate and eventually leads to formaldehyde and formic acid cannot be ruled out since both are products of reaction path D.

The last reaction sequence (D) indeed seems to be a domi-

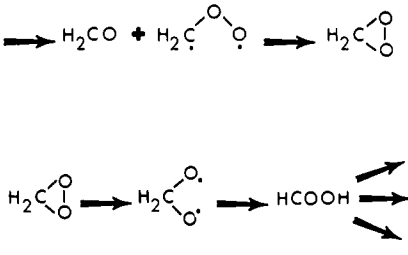

(D)

nant route since dioxirane has been observed and its decomposition leads to the expected end products H_2 and CO.[25]

C. Dioxirane Derivatives. As discussed in the previous paper,[13] dioxirane is found in the reaction of ozone with other terminal olefins (propene, 1-butene, and vinyl fluoride). The branching evidenced with the observation of formaldehyde suggests that substituted dioxiranes should also be formed in the reaction although we were unable to observe them. This

is probably the result of unfavorable vapor pressure versus decomposition temperature behavior.

The substituent groups, F, CH_3, or C_2H_5 most likely would not substantially increase the strength of the O-O bond, while they would reduce the volatility of the substituted dioxirane compared with that of dioxirane itself. If this is true, a more sensitive technique is required to observe these species in the gas phase, although spectral studies of these species in the condensed phase might be the best means of characterizing them.

Hull et al.[10] reported a low-temperature infrared study of alkene-ozone reactions with the products in the condensed phase. They assigned a number of new infrared bands by assuming the product was 1,2,3-trioxolane (primary ozonide) and measured the decomposition temperature of the new species for each of the olefins employed. In the case of ethylene they report a decomposition temperature in the range −100 to −80 °C which is strikingly similar to that determined for dioxirane.[13,25] If indeed the infrared bands detected by Hull et al. arose from dioxirane or its derivatives, their measured decomposition temperatures indicate that the derivatives are less stable than dioxirane. Clearly more work is needed to better characterize the products of low-temperature ozone-olefin reactions.

Acknowledgment. The authors gratefully acknowledge C. V. Kurtz for construction of the absorption cell and assisting in the measurements. Support for this work was provided by the Office of Air and Water Measurements of the National Bureau of Standards.

References and Notes

(1) C. Harries, *Chem. Ber.*, **36**, 1933 (1903).
(2) H. Staudinger, *Chem. Ber.*, **58**, 1988 (1925).
(3) R. Criegee, *Rec. Chem. Prog.*, **18**, 111 (1957).
(4) (a) P. R. Story, R. W. Murray, and R. D. Youssefyeh, *J. Am. Chem. Soc.*, **88**, 3144 (1966); (b) R. W. Murray, R. D. Youssefyeh, and P. R. Story, *ibid.*, **89**, 2429 (1967); (c) R. W. Murray, *Acc. Chem. Res.*, **1**, 313 (1968).
(5) N. L. Bauld, J. A. Thompson, C. E. Hudson, and P. S. Bailey, *J. Am. Chem. Soc.*, **90**, 1822 (1968).
(6) R. P. Lattimer, R. L. Kuczkowski, and C. W. Gillies, *J. Am. Chem. Soc.*, **96**, 348 (1974).
(7) P. A. Leighton, "Photochemistry of Air Pollution", Academic Press, New York, N.Y., 1961.
(8) C. W. Gillies and R. L. Kuczkowski, *J. Am. Chem. Soc.*, **94**, 6337 (1972).
(9) F. L. Greenwood and L. J. Durham, *J. Org. Chem.*, **34**, 3363 (1969).
(10) L. A. Hull, I. C. Hisatsune, and J. Heicklen, *J. Am. Chem. Soc.*, **94**, 4856 (1972).
(11) D. R. Johnson and R. Pearson, Jr., in "Methods of Experimental Physics", Vol. 13, Academic Press, New York, N.Y., 1976, pp 102-133.
(12) G. A. Cook, A. D. Kiffer, C. V. Klumpp, A. H. Malik, and L. A. Spence, *Adv. Chem. Ser.*, **No. 21**, 44 (1959).
(13) F. J. Lovas and R. D. Suenram, *Chem. Phys. Lett.*, **51**, 453 (1977).
(14) J. G. K. Watson, *J. Chem. Phys.*, **46**, 1935 (1967).
(15) W. H. Kirchhoff, *J. Mol. Spectrosc.*, **41**, 333 (1972).
(16) C. C. Costain, *J. Chem. Phys.*, **29**, 864 (1958).
(17) J. Kraitchman, *Am. J. Phys.*, **21**, 17 (1953).
(18) A. Chutjian, *J. Mol. Spectrosc.*, **14**, 361 (1964).
(19) The equations derived by Chutjian have been simplified somewhat by L. Nygaard, *J. Mol. Spectrosc.*, **62**, 292 (1976).
(20) J. M. L. J. Reinartz and A. Dymanus, *Chem. Phys. Lett.*, **24**, 346 (1974).
(21) S. Golden and E. B. Wilson, *J. Chem. Phys.*, **16**, 669 (1948).
(22) J. Callomen, B. Hirota, K. Kuchitsu, W. Lafferty, A. Maki, and C. Pote, "Structure Data of Free Polyatomic Molecules", Group II, Vol. 7, Landolt-Börnstein, Springer-Verlag, Berlin, 1976.
(23) T.-K. Ha, H. Kühne, S. Vaccani, and Hs. H. Günthard, *Chem. Phys. Lett.*, **24**, 172 (1974).
(24) W. R. Wadt, and W. A. Goddard III, *J. Am. Chem. Soc.*, **97**, 3004 (1975).
(25) R. I. Martinez, R. E. Huie, and J. T. Herron, *Chem. Phys. Lett.*, **51**, 457 (1977).
(26) L. B. Harding and W. A. Goddard III, *J. Am. Chem. Soc.*, in press.
(27) H. Kühne, S. Vaccani, T.-K. Ha, A. Bauder, and Hs. H. Günthard, *Chem. Phys. Lett.*, **38**, 449 (1976).

Spectroscopic Properties of Cyclic and Bicyclic Azoalkanes

Manfred J. Mirbach,[1a] Kou-Chang Liu,[1a] Marlis F. Mirbach,[1a] William R. Cherry,[1a] Nicholas J. Turro,*[1a] and Paul S. Engel*[1b]

Contribution from the Department of Chemistry, Columbia University, New York, New York 10027, and the Department of Chemistry, Rice University, Houston, Texas 77001. *Received July 11, 1977*

Abstract: The spectroscopy and photochemistry of 19 cyclic azoalkanes have been investigated. The absorption spectra consist of a (usually structured) band in the region of 300-400 nm (ϵ 100-600 L/(cm mol)) which is assigned to a (n_-,π^*) transition. Fluorescence is readily detected from most of the azoalkanes examined, but the fluorescence quantum yields vary from nearly 1.0 to 10^{-4} depending upon azoalkane structure as well as the solvent. The absorption maxima show a blue shift and the emission maxima a red shift as solvent polarity increases. For representative examples, the rate constants for photochemical nitrogen extrusion have been determined. These values were found to correlate with the lowest ionization potential of the azoalkane (n_- MO). Finally, the effect of solvent on the fluorescence quantum yields and fluorescence lifetimes were determined. The results are rationalized within the framework of conventional quenching mechanisms.

Introduction

Although the photochemistry of cyclic azoalkanes has been widely studied[2a,b] only a few systematic investigations have been carried out on their spectroscopic behavior.[2c] Cyclic azoalkanes commonly exhibit fluorescence, in contrast to their acyclic counterparts. The (usually) highly structured absorption and emission spectra and the absence of side reactions which compete with fluorescence and loss of nitrogen (e.g., cis-trans isomerization or tautomerization) make the cyclic azoalkanes (**1-19**) (Scheme I) attractive models for a systematic spectroscopic and photochemical investigation. In this paper we report a detailed study of the spectroscopic properties of compounds **1-19**.

Experimental Section

The structures of the azoalkanes investigated in this work are given in Scheme I. Samples of **10, 13, 14,** and **15** were obtained from Professors C. Steel,[3] B. Jacobson,[4] E. L. Allred,[5] and T. J. Katz,[6] respectively. The other azoalkanes were prepared as previously described. For compound **1b** see ref 7; for compounds **2** and **3** see ref 8; for compounds **4-9** and **11** see ref 9, for compounds **16-19** see ref 11, 12, 13a, and 13b, respectively; and for compound **12** see ref 10.

Absorption spectra were measured on a Cary 17 spectrometer. The

0002-7863/78/1500-5122$01.00/0